https://doi.org/10.5194/egusphere-2024-3331
Preprint. Discussion started: 15 November 2024

Saharan warm air intrusions in the Western Mediterranean: identification, impacts on temperature extremes and large-scale mechanisms

Pep Cos[1,2], Matias Olmo[1], Diego Campos[1,2], Raül Marcos-Matamoros[2], Lluis Palma[1,2], Ángel G. Muñoz[1], and Francisco J. Doblas-Reyes[1,3]

[1]Earth Sciences Department, Barcelona Supercomputing Center (BSC), Barcelona, Spain
[2]Department of Applied Physics, University of Barcelona, Barcelona, Spain
[3]Institució Catalana de Recerca i Estudis Avançats (ICREA), Barcelona, Spain

Correspondence: Pep Cos (josep.cos@bsc.es)

Abstract. Saharan warm intrusions are air masses that develop over the Saharan region and that get advected into surrounding regions, creating anomalous atmospheric situations in other regions. This paper focuses on the characteristics of these intrusions into the Western Mediterranean region (WMed) and their relationship with extreme temperatures in the neighbouring areas during the recent past (1959-2022). We describe and evaluate a methodology to identify Saharan air masses throughout the year and, consequently, a historical catalogue of intrusion events that reach the WMed is built. To identify which large-scale phenomena might be relevant for the formation of the intrusions, we first identify different intrusion types (IT) through a clustering procedure. Four different ITs are found, which discriminate the intrusions according to their longitudinal position over the Mediterranean region. Upper-tropospheric anomalies are linked to the onset of these events, in particular, an anomalous geopotential high over the intrusions region that slows down the upper-tropospheric circulation over northern Africa. These events are very relevant as they impact extreme temperatures throughout the year and account for a high percentage of the extreme temperature events recorded in the WMed and neighbouring regions in summer.

1 Introduction

Numerous studies discussing the Mediterranean climate have underscored important changes in temperature, precipitation, and their extremes (Lionello and Scarascia, 2018; Giorgi, 2006; Cos et al., 2022; Olmo et al., 2024), with significant impacts on ecosystems, economies, and humans (Seager et al., 2019; Cherif et al., 2020; Cramer et al., 2018). In the context of climate change, it is crucial to develop robust methods for estimating the future state of the Mediterranean climate. Confidence in model projections depends on, among other things, our understanding of the physical mechanisms driving the observed climate (Barriopedro et al., 2023). To interpret both observational data and climate model simulations effectively, researchers have worked to unravel the physical processes that shape climate patterns. In the case of the Mediterranean some studies have focused on the drivers behind the mean state of temperature and precipitation (Tuel and Eltahir, 2020; Brogli et al., 2019;

https://doi.org/10.5194/egusphere-2024-3331
Preprint. Discussion started: 15 November 2024

Bladé et al., 2012), while others have explored the mechanisms behind climatic-impact drivers like heatwaves and extremes, analysing both large-scale circulation and interaction of climate modes of variability (Alvarez-Castro et al., 2018; Faranda et al., 2023; Horton et al., 2015; Muñoz et al., 2015, 2016, 2017) and local processes (Materia et al., 2022; Vogel et al., 2017; Urdiales-Flores et al., 2023; Nabat et al., 2015). Yet, some climate processes and phenomena require further investigation to improve our ability to predict, communicate, and adapt to present and future changes in the Mediterranean climate. Among those phenomena, intrusions of warm air masses that form in the Sahara and get advected northward (Sousa et al., 2019) have received particularly scarce attention.

There is a large body of literature about Saharan dust intrusions in the Mediterranean, which are very relevant for air quality and human health. However, the climatological properties of the intrusions of warm air, which might be accompanied, or not, by Saharan dust, are not well known. And this is in spite of indications of authors like Sousa et al. (2019), who suggested that warm air intrusions from the Sahara can be a driver of heat waves in the Iberian Peninsula. Some work exists for summer intrusions (Sousa et al., 2019; Galvin, 2016), although here we aim to generalise the definition for the whole year. Further work is required to obtain a wider picture of what a Saharan warm air intrusion is and what its implications on the broader Western Mediterranean temperature extremes are. We aim at widening the scope of the Saharan intrusions studies by focusing primarily on temperature, rather than on the far more studied dust storm and transport phenomenon (Cuevas-Agulló et al., 2023).

Sousa et al. (2019) studied the impact that past intrusion events have on heat waves in the Iberian Peninsula and Pereira et al. (2005) demonstrated the effect that advections from northern Africa can have on Portugal forest fires. These case studies made us wonder what the impact and contribution of an intrusion in generating extreme temperature days is and what the spatial extent of its area of influence is. Besides, from a large-scale perspective the question of what synoptic situations lead to those intrusions emerges. We think that, apart from describing their climatological characteristics, it is important to link the Saharan intrusions both to the impact they have on temperature and to the larger scale circulation that is associated with their onset.

In order to better understand the phenomenon and its processes from a climatological point of view, an objective identification algorithm for these masses is required. The algorithm would allow us to build a historical catalogue of events that can be used to gain insight on the phenomenon, its impacts and characteristics. Moreover, this identification and assessment framework should be easily applied to climate model simulations to evaluate the model ability at reproducing intrusions. Potentially this could contribute to implementing process-based constraints in climate models (Palmer et al., 2023; Regayre et al., 2023; Fasullo and Trenberth, 2012). To identify warm air intrusions, we will focus on the thermodynamic properties that define air masses formed at low-latitude subtropical desertic areas.

This study has four objectives to characterise Saharan air intrusions into the Western Mediterranean (WMed henceforth) during the recent historical period:

(a) Generalise the definition of a Saharan warm air intrusion.

(b) Describe the characteristics of the intrusions: spatial distribution, seasonality, etc.

(c) Assess the impact and contribution of the intrusions to extreme temperatures in the Euro-Mediterranean region.

https://doi.org/10.5194/egusphere-2024-3331
Preprint. Discussion started: 15 November 2024

(d) Study which large-scale phenomena may play a predominant role in the development of warm-air intrusions.

The paper, after presenting the data used for the analyses in Section (2), presents a series of sections that establish the criteria to identify and assess Saharan intrusions in the WMed in the historical period. The structure is as follows:

- Section 3 describes a methodology to identify Saharan air masses.
- Section 4 assesses the differences between intrusions and defines different intrusion types through a clustering algorithm.
- Section 5 illustrates different characteristics of the intrusions and their relationship with extreme temperatures in the Euro-Mediterranean region.
- Section 6 proposes links between the large-scale circulation and the Saharan warm air intrusions.

We present an easily reproducible workflow to support future work in understanding the phenomenon and to evaluate the capacity of climate models to reproduce the Saharan intrusions.

2 Data

In this study, we use both surface and pressure-level observationally-based data in the historical period at a daily scale. We employ daily means from 1-hourly data of the ERA5 reanalysis from years 1959 to 2022 at 0.25ºx0.25º resolution (Hersbach et al., 2020). The variables used to define and identify warm-air intrusions are air temperature at 925 and 750 hPa, and geopotential height at 1000 and 500 hPa. Composites of the intrusion days are computed for geopotential height and wind speeds at different levels (850 hPa, 300 hPa and 500 hPa; the latter not shown). Daily maximum temperature (TX) is used to identify the relationship between Saharan intrusion events in WMed and extreme temperatures in the Euro-Mediterranean region.

3 Saharan air mass definition and intrusion catalogue

First we define some indicators to detect Saharan air masses. We took a definition of a Saharan air mass in summer from the work of Sousa et al. (2019) that allowed the authors to identify the intrusions of June 2018 and August 2019. This definition takes into account both the temperature and vertical homogeneity of a column of warm air characteristic of the latitude and surface radiative balance in the Sahara desert (Webster, 2020). Two indicators can inform us about these air mass characteristics: the geopotential thickness between levels 1000 and 500 hPa ($\Delta GH_{500-1000}$, henceforth) and the average potential temperature between levels 925 and 750 hPa ($\overline{\theta}_{750-925}$). From Sousa et al. (2019); Galvin (2016); Webster (2020), the summer (June–August) thresholds are suggested to be around 5300 m and 40ºC, respectively, which are based on the climatological

https://doi.org/10.5194/egusphere-2024-3331
Preprint. Discussion started: 15 November 2024

mean summer values of air masses of subtropical origin.

$$\overline{\theta}_{750-925} = \frac{\theta_{925} + \theta_{750}}{2} \text{ ; where } \theta = T(\frac{1000}{P})^{\frac{R_d}{C_p}} \quad (1)$$

and

$$\Delta GH_{500-1000} = GH_{500} - GH_{1000} \quad (2)$$

where θ_i is the potential temperature at the pressure level i (in hPa), T is the temperature, P is the pressure, R_d is the gas constant, C_p is the specific heat at constant pressure and GH_i is the geopotential height at pressure level i.

By conducting a study of the monthly climatologies of the two indicators, we find that the Sahara desert behaves, in the warm months, differently to the cold ones (see Supplementary Figure S1). The indicators in the Sahara region during the warm months have maximum values compared to any surrounding region, while during the cold season $\Delta GH_{500-1000}$ and $\overline{\theta}_{750-925}$, have an almost constant latitudinal gradient in the longitudinal band 15ºN-35ºN,30ºW-50ºE. We take as representative of the Sahara desert the red box in Figure 1 throughout the year, which leads to climatologies close to those defined by other studies (Galvin, 2016; Sousa et al., 2019; Webster, 2020). Figure 2 shows the pool of data from all points within the Saharan and WMed (defined as the blue box in Figure 1) for all days between 1959 and 2022, which indicates the monthly historical values of the indicators in each region and shows how far away they are from each other. In Figure 2 we see that the monthly-mean Saharan air mass, represented by the mean $\Delta GH_{500-1000}$ and $\overline{\theta}_{750-925}$ (red lines), is an extreme in the WMed distribution.

As we aim to identify Saharan air masses for other seasons beyond the summer, we find daily thresholds for $\Delta GH_{500-1000}$ and $\overline{\theta}_{750-925}$ by computing the climatology of the indicators over the Saharan region for each 31-day rolling window of the year. For an example in May of 2015, thresholds are indicated in dashed green and cyan lines in Figure 1. When they coincide, the area is red shaded to represent a Saharan air mass. The rolling thresholds vary smoothly and allow the identification of continuous events along the year. To consider any day as an intrusion day, the Saharan air mass (red shading in Figure 1) must cover a sufficiently large area within the WMed, which is taken to be 5% of the region (dashed black box in Figure 1).

To make sure that the events detected are not air masses formed away from the Sahara, a visual inspection of all the event days is performed, verifying that the definition holds: all intrusion events represent air masses that are displaced northward from the Saharan region. There are differences between May-October Saharan air masses and November-March ones. During the warmer months (May-October), the thermodynamic properties of the air masses in the Sahara are distinctive, i.e. the heat of the column of air is larger than in any region surrounding the areas that span from the Sahara to the east of the Arabian peninsula. During the cold months (November-March), the thermodynamic properties of the air over the Sahara are not so different from the surrounding regions. In fact, we observe a latitudinal gradient in both indicators that is consistent across all longitudes shown in Figure S1, i.e. between the latitudes encompassing the Sahara region (red box) from the Atlantic (at 30º W) to Arabia (50º E).

https://doi.org/10.5194/egusphere-2024-3331
Preprint. Discussion started: 15 November 2024

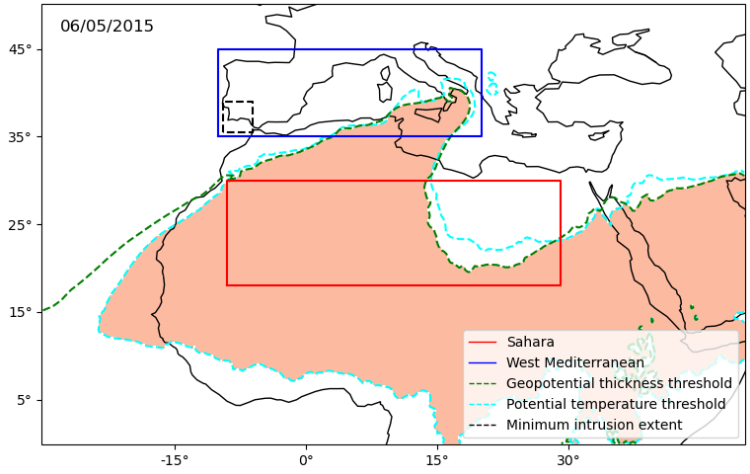

Figure 1. The map shows the intrusion situation of May 5th 2015, when a Saharan air mass entered along the western boundary of the WMed. The WMed (blue) and the Saharan regions used to compute the thresholds (red) are enclosed by boxes. The dashed green and cyan lines are the boundaries of the region where the geopotential thickness between 1000-500 hPa and average potential temperature between 925-750 hPa, respectively satisfy the criteria for the air mass to be considered a Saharan air mass. The shaded orange region is the area where the two thresholds are met simultaneously. The dashed black box illustrates the minimum area inside the WMed that must be under Saharan air conditions to consider a day as an intrusion day (this area can be located anywhere within the WMed).

Through this identification algorithm, a catalogue (Figure S2) is obtained for the 1959-2022 period, showing that the months with most of the intrusions are July and August, as well as December. There is also some notable activity during January-February and May-June. During early spring and autumn the amount of intrusions is reduced.

We now focus on a particular event from this catalogue for a better understanding of the vertical properties of the Saharan air masses that move into the WMed. Figure 3 shows the daily mean fields and vertical sections during an event in August of 2006. From Figure 3, we can see how a mass penetrates south of Sardinia (37.5º N 17º E) driven by an intense trough developed in the North Atlantic. The vertical profiles of potential temperature show that the intruded mass has distinct features with respect to the surrounding areas. In the regions where Saharan air masses are identified, the vertical profiles show high potential temperatures, indicating that the mass comes from lower latitudes (or a region where it could warm up); the vertically-homogeneous daily-mean potential temperature in the latitudinal and longitudinal cuts indicates the predominance of mixing by convection. This agrees with the properties of air masses formed above desertic areas, where the surface long wave radiation can lead to convection and to a very warm and homogeneous air column (Webster, 2020). The reader is referred to Supplementary Figures S3 and S4 that show two more events that also illustrate the properties of a Saharan air mass.

https://doi.org/10.5194/egusphere-2024-3331
Preprint. Discussion started: 15 November 2024

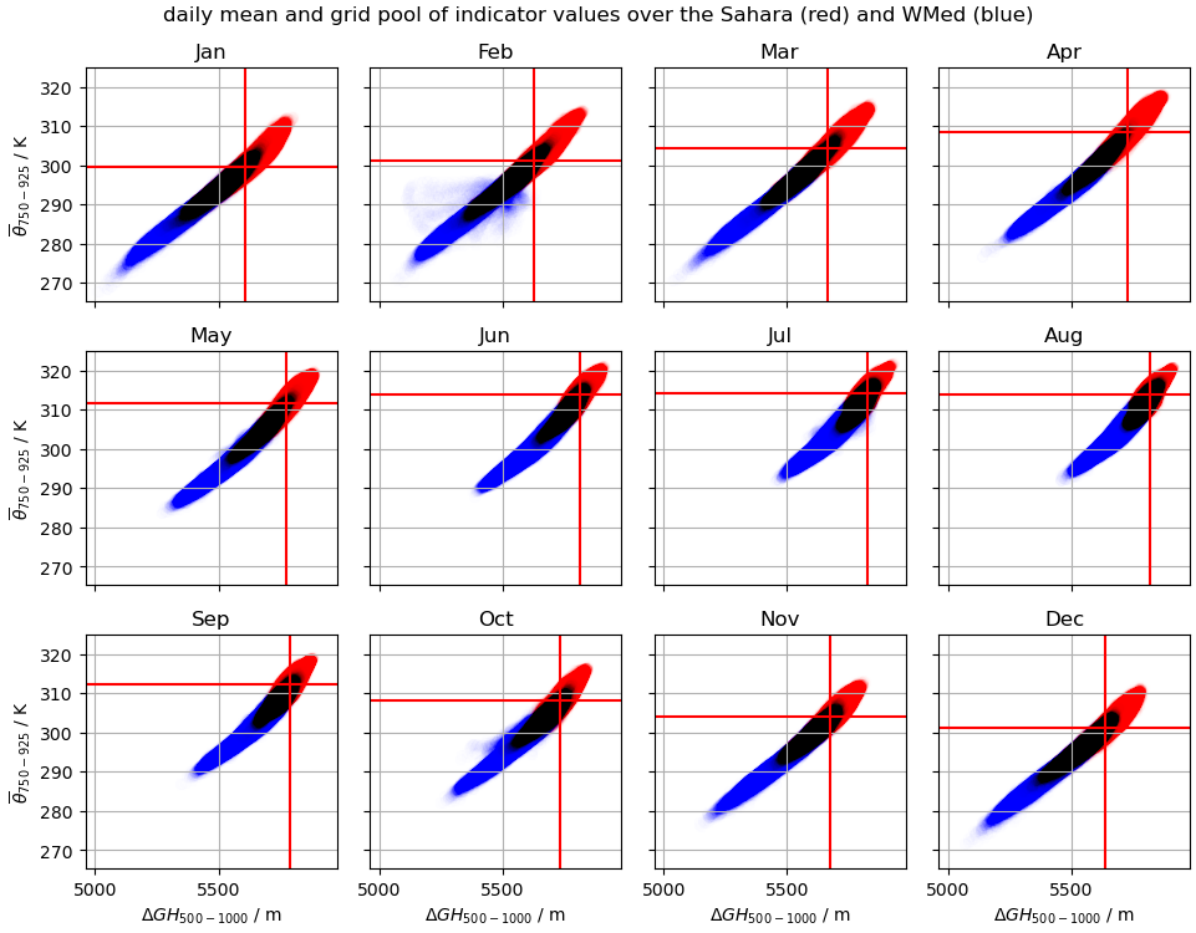

Figure 2. Monthly (different panels) pool of $\Delta GH_{500-1000}$ and $\overline{\theta}_{750-925}$ values over the whole grid points and days in the Western Mediterranean (blue) and the Sahara (red) regions for the period 1959-2022. The red lines show the Sahara climatologies. The black area shows overlap values between the Sahara and WMed.

4 Intrusion types

The visual inspection of individual events is informative, but lacks some generalisation to allow a climatological study of the events. Therefore, we aim to classify the intrusions according to their different expressions. The intrusions present local features that span smaller spatial scales than the whole WMed. This would suggest that different types of intrusion might exist depending on the area where they develop in the study region.

A clustering methodology is employed to make an initial classification of the different intrusions. To account for differences in the radiative forcing, atmospheric circulation and thermodynamics in the Sahara along the year, we apply a clustering analysis of the intrusion events in each meteorological season (DJF, MAM, JJA and SON, henceforth). Our approach employs the

https://doi.org/10.5194/egusphere-2024-3331
Preprint. Discussion started: 15 November 2024

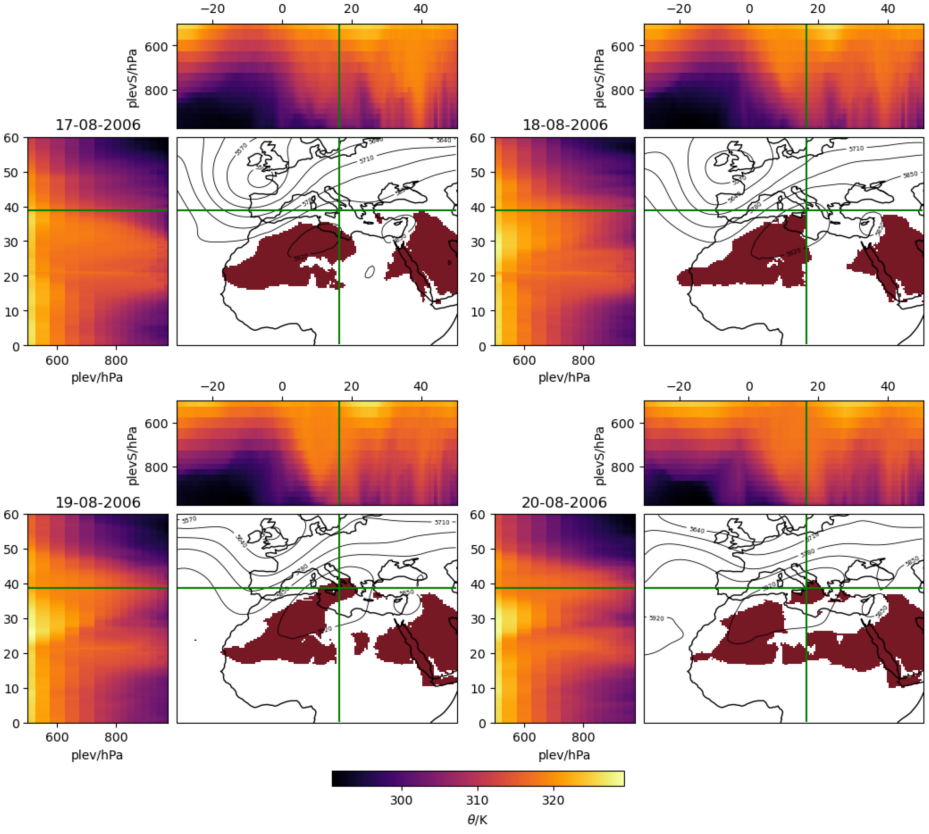

Figure 3. Intrusion event observed in the period 17/08/2006 to 20/08/2006. The panels show the daily situation before, during and after the event. The air mass identified as Saharan is shaded red while the contours show the geopotential height at 500 hPa. The sub-panels to the left and top of the maps correspond to the vertical sections between pressure levels (plev) 975-500 hPa of potential temperature along the vertical and horizontal green lines.

$\Delta GH_{500-1000}$ and $\overline{\theta}_{750-925}$ indicators during intrusion days in the WMed as input in a clustering procedure. The method is a combination of a reduction of the dimensionality via S-Mode principal components analysis (99% of the spatial variance is maintained) and the k-means clustering of the matrix of stacked indicators, similar to (Tencer et al., 2016; Muñoz et al., 2015, 2016, 2017; Olmo et al., 2024).

A sensitivity analysis is performed to determine the optimal number of clusters, using both the Silhouette score (Rousseeuw, 1987) and the Pseudo-F metric (Calinski and Harabasz, 1974). The Silhouette score is calculated for each data sample based on the mean intra-cluster distance (the average distance within a cluster) and the mean nearest-cluster distance (the average distance to the nearest cluster). The Pseudo-F score is computed by dividing the between-cluster sum of squares (which measures the dispersion between cluster centroids) by the within-cluster sum of squares (which measures the dispersion of data points within their assigned clusters). Together, these metrics provide insight into the clustering structure. However, neither

https://doi.org/10.5194/egusphere-2024-3331
Preprint. Discussion started: 15 November 2024

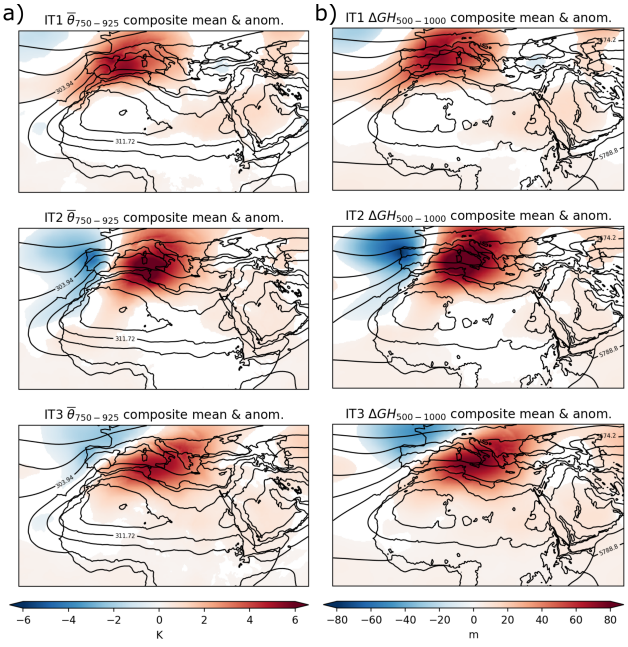

Figure 4. June-to-August composites of anomalies with respect to the mean climatology of the days without intrusion for $\overline{\theta}_{750-925}$ (a) and $\Delta GH_{500-1000}$ (b) for the three clusters. Solid contours display the climatological values not accounting for intrusion days.

metric indicates a clear optimal number of clusters, likely due to the high variability of the indicators during intrusion days. To address this issue, we prioritise relative maxima in the Silhouette scores that coincide with an elbow in the Pseudo-F curve, which allows us to synthesise as much as possible the number of clusters (intrusion types, IT). The resulting number of ITs are 5 for DJF, 3 for JJA and 4 for MAM and SON (see Figure S5). Finally, each intrusion day is assigned to a centroid according to the Euclidean distance between the indicator fields of each day and the centroid.

Results obtained from clustering the intrusion days for $\overline{\theta}_{750-925}$ and $\Delta GH_{500-1000}$ over the WMed show that the ITs can be distinguished by the location where the anomalously warm air mass is found. Figure 4 shows the $\Delta GH_{500-1000}$ and $\overline{\theta}_{750-925}$ composites for the JJA ITs. They show a distribution between western, central and eastern WMed. Supplementary Figure S5 shows the rest of the seasons. MAM and SON display similar characteristics but dividing the region into four longitudinal bands. DJF also has longitudinal separations, but some latitudinal differences appear, suggesting that different ITs are also clustered in terms of how much they can move northward. We introduce the term "area of influence" of each IT as the anomalously warm region seen in Figures 4 and S6.

Figure 5 shows the JJA intrusion days colour-coded according to the IT they belong to (see Figure S7 for the other seasons). During persistent events, the IT can either remain constant or transition, meaning that the Saharan air mass can remain stationary in the IT area of influence or move towards other regions. In JJA and SON, there is a significantly positive trend (See Figure 6a,c) in the number of intrusion days per year and season (blue bars), and the mean persistence of the events is quite constant for all seasons (orange bars).

https://doi.org/10.5194/egusphere-2024-3331
Preprint. Discussion started: 15 November 2024

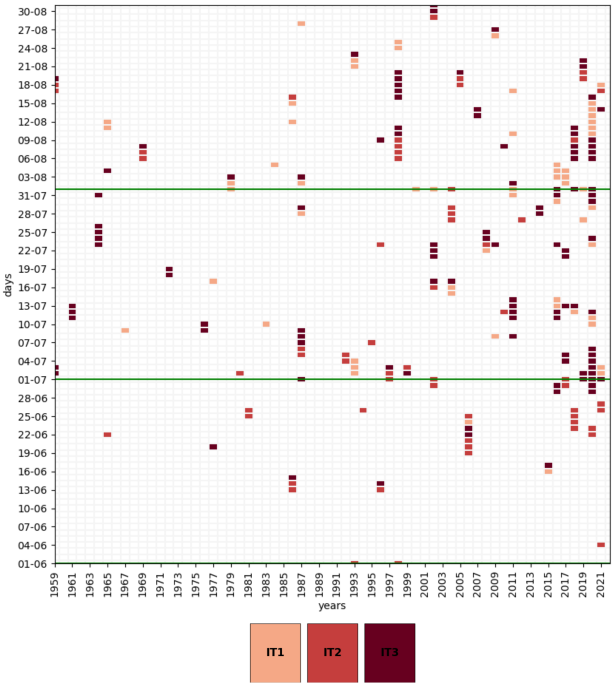

Figure 5. Historical catalogue of intrusion days in the period 1959-2022 (x-axis) and from the 1st of June to the 30th of August (JJA, y-axis). The days identified as intrusions are coloured with their assigned IT. Green lines indicate the change of months.

Given that intrusion days can shift from an IT to another, the transition probability heatmaps are computed (see Figure S8). They inform about the persistence or changes in the IT between one day and the next one. ITs are generally persistent in JJA, although IT1 can transition often to IT2 and IT3. DJF shows very little persistence, and MAM and SON show mixed behaviours depending on the IT. Kendall-tau (τ) correlations have been computed between the yearly intrusion days of every IT (labelled as ID) and some relevant teleconnection indices in the region. While the association values are low, statistically significant relationships at the 95% level have been found for the Atlantic Multidecadal Oscillation (Klotzbach and Gray, 2008), the Arctic Oscillation (Thompson and Wallace, 1998) and the Western Mediterranean Oscillation (Martin-Vide and Lopez-Bustins, 2006):

- $\tau(ID^{\text{JJA}}_{\text{IT2}}, AMO_{\text{JJA}}) = 0.26$
- $\tau(ID^{\text{JJA}}_{\text{IT3}}, AMO_{\text{JJA}}) = 0.20$
- $\tau(ID^{\text{DJF}}_{\text{all IT}}, AO_{\text{DJF}}) = -0.20$
- $\tau(ID^{\text{DJF}}_{\text{all IT}}, WeMO_{\text{DJF}}) = 0.22$

https://doi.org/10.5194/egusphere-2024-3331
Preprint. Discussion started: 15 November 2024

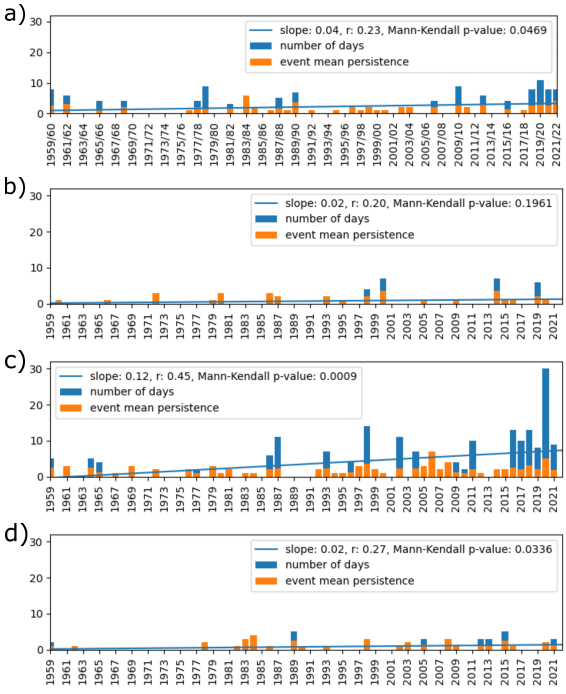

Figure 6. Number of identified Saharan warm air intrusions in a) DJF, b) MAM, c) JJA and d) SON per year between 1959-2022 (blue bars). The mean duration of each intrusion event, from the first to the last continuous day, is shown with orange bars. A least squares linear regression fit to the seasonal number of intrusion days is shown in blue.

5 Intrusions and extreme temperatures in the Euro-Mediterranean region

In this section we focus on the broader Euro-Mediterranean region (EM, henceforth) and assess the influence of intrusions on extreme temperatures. We compute the number of warm days at each grid cell, estimated as those days that exceeded their 7-day rolling mean climatological 90th percentile (TX90p) (Zhang et al., 2005; Wang et al., 2013). We define the impact and contribution to extreme temperatures for each IT and season as:

$$Impact = P(TX90p \mid \text{intrusion day}) = \frac{P(TX90p \cap \text{intrusion day})}{P(\text{intrusion day})} \tag{3}$$

$$Contribution = P(\text{intrusion day} \mid TX90p) = \frac{P(\text{intrusion day} \cap TX90p)}{P(TX90p)} \tag{4}$$

where $P(TX90p \mid \text{intrusion day})$ is the probability of having an extreme temperature day (TX90p) given that the day is also an intrusion day (i.e. the intrusion impact) and $P(\text{intrusion day} \mid TX90p)$ is the probability of having an intrusion day in the

https://doi.org/10.5194/egusphere-2024-3331
Preprint. Discussion started: 15 November 2024

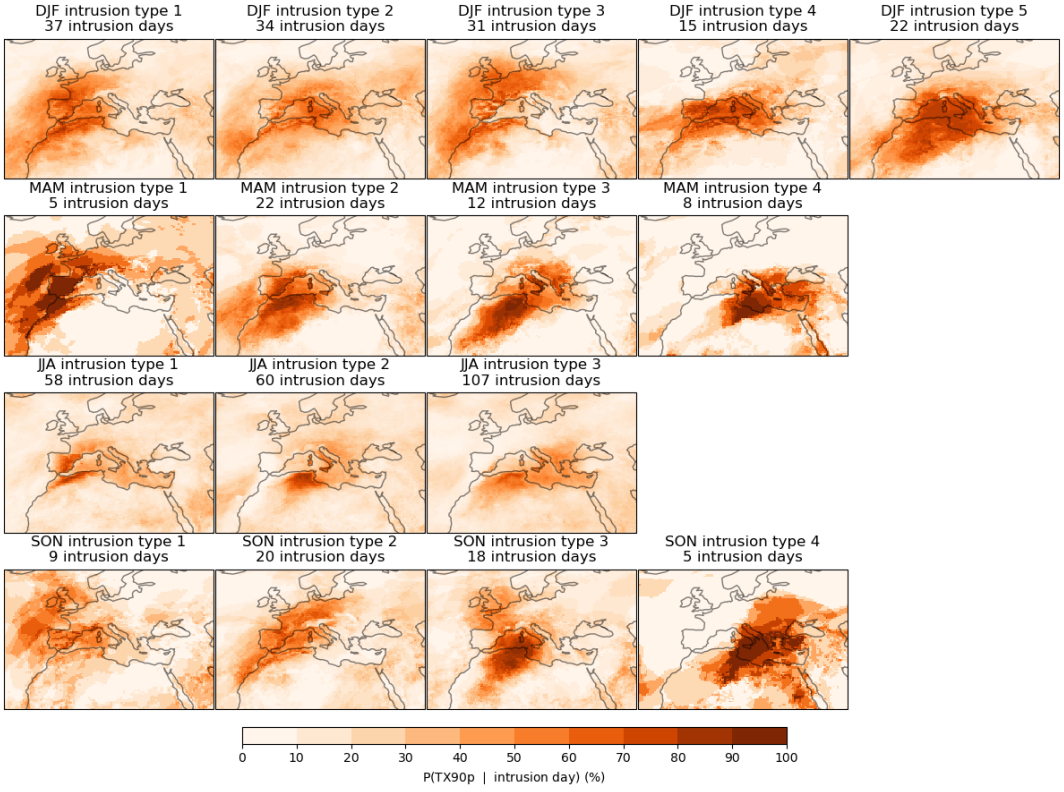

Figure 7. Impact of the Saharan warm air intrusions on extreme temperatures in the EM region for the different seasons (rows) and ITs (columns). The impact is measured as the percentage of intrusion days that coincide with an extreme temperature day (TX90p). The amount of intrusion days for each season and IT is specified in the title of each panel.

sample of TX90p days (i.e. contribution of the intrusion to extreme temperatures).

The impact of Saharan intrusions on temperature extremes in the EM depends on the season and on the IT (see Figure 7). The reader will note that some of the results come from a small number of intrusions (depending on the season). Nonetheless, the results are important as they highlight the impact of those events (the number of days are provided in the top of each panel). During DJF, MAM and SON, Saharan intrusions can have an impact on regions beyond the WMed. Contrarily, during JJA, the impact is quite confined to the area of influence of each IT. We assess the results for the first and second days after the end of the intrusion events and we see impacts in extreme temperatures although lower than during intrusion days. Also, the impacts after the events end are generally shifted eastward from the area of influence of each IT, in line with the westerly circulation in the region (see Supplementary Figure S9).

Regarding the contribution of Saharan warm air intrusions to extreme temperatures, we see from Figure 8 that the largest contributions come from JJA, with values of around 10% of the TX90p days. The spatial extent is rather confined to the ITs

https://doi.org/10.5194/egusphere-2024-3331
Preprint. Discussion started: 15 November 2024

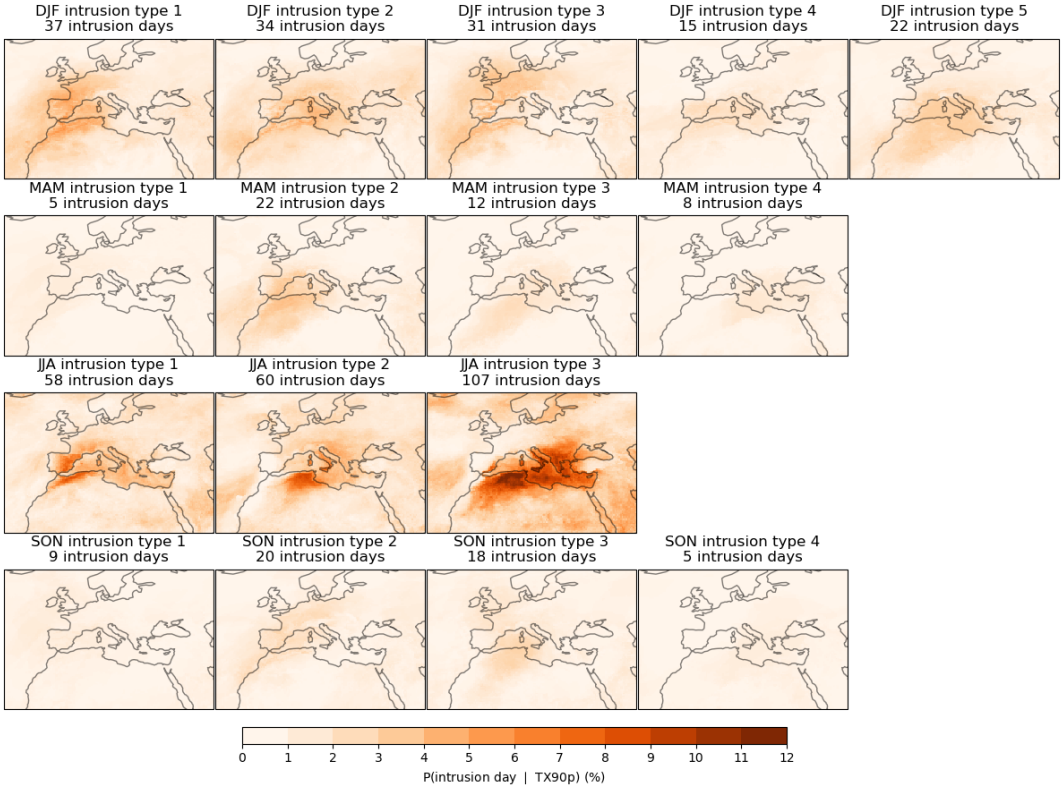

Figure 8. Contribution of the Saharan warm air intrusions to the extreme temperature days (TX90p) of each season (rows) and IT (columns). The contribution is calculated as the percentage of extreme temperature days that coincide with a Saharan intrusion.

area of influence, although the relevant contributions of IT3 reach further east. Other seasons present much lower contributions, mainly due to the lesser number of intrusion days in the catalogue. DJF can reach up to contributions of 5% of warm days, and the spatial extent goes from northern Africa to the south bound of northern Europe.

To illustrate the differences between impact and contribution we focus on SON: Figure 7 shows that SON intrusions have an important impact in producing extreme events, meaning that most intrusion days produce TX90p temperatures in the area of influence and beyond; nevertheless, Figure 8 shows that SON intrusions contribute very little to all the TX90p days in the season, mainly because there are few intrusion days during SON.

6 Large-scale circulation associated with the intrusion onset

Composites for each IT can be computed for any meteorological variable. This becomes helpful to understand the anomalies during intrusion days. First, we need the anomalies of any variable of interest, which are computed by subtracting the non-

https://doi.org/10.5194/egusphere-2024-3331
Preprint. Discussion started: 15 November 2024

intrusion climatologies of 7-days moving windows centred on each calendar day (Zhang et al., 2011; Tencer et al., 2016; Olmo et al., 2020). For example, we compute the upper-tropospheric geopotential height composites of any IT by first calculating the non-intrusion climatologies (using a 7-day running average), subtracting them to the intrusion days composite and then averaging these anomalies for the intrusion days. We are particularly interested in the relationship between the circulation and the onset of the intrusion events. Therefore, the composites are from the first day of the intrusion events. The results help to identify the mechanisms behind the intrusions.

In previous analyses, we saw that the different ITs are related to where the intrusion is located in the WMed (Figure 5). This result is reinforced by Figure 9-10,b (from DJF and JJA, respectively) and S10-S11,b (from MAM and SON, respectively), which shows the anomalous winds at 850 hPa for each IT. Masked areas mean that the anomalies are not significantly different from zero according to a two-tailed 95% confidence t-test (Ukkola et al., 2020). The northward wind anomalies coincide with the areas of impact of the ITs meaning that there is an advection of southern air into the WMed. Figure 9-10,b and S10-S11,b also show the anomalies in sea-level pressure (SLP) in shading, and for most of the ITs there is an associated low pressure located to the west/northwest, north or northeast from the area of influence. Some ITs do not have a clear statistically significant SLP anomaly signal (DJF IT3 and SON IT2). Overall, the low-tropospheric circulation and the SLP anomalies are coherent.

When looking into the mid/upper-troposphere ($\tilde{3}$00 hPa), very well defined and significant anomalies are detected both in wind speeds and geopotential height (see Figure 9-10,a and S10-S11,a). Generally, there is alway a statistically significant and well defined geopotential high over the area of influence of the intrusion. Most times this high is accompanied by a low that is located to the west, northwest, north or northeast. This anomalous negative geopotential centre is generally well aligned vertically with the negative sea level pressure (although some ITs present some baroclinicity). The winds in the upper troposphere are consistent with the geopotential centres, suggesting that the general circulation (westerlies) is slowed down south of the geopotential positive blob, which can lead to onsets of intrusion events. The main differences between seasons is that the anomaly centres in DJF are generally broader and more intense than in JJA. MAM and SON composites have similar behaviours and also show broad and intense anomaly centres but to a lesser extent than DJF.

The composites of the days leading to the intrusion onset (Figures S12-S13) show that the anomalies in the upper troposphere generally propagate over the North Atlantic (in DJF, with large spatial extents) and in the eastern North Atlantic (in JJA, with smaller spatial extents), first as a deepening trough (negative geopotential anomaly at 300hPa) that leads to a high over the area of influence of the IT.

7 Discussion and conclusions

This study aims at characterising Saharan warm air intrusions into the western Mediterranean, as the limited literature suggests that these events significantly influence extreme temperatures in the region (Sousa et al., 2019). Our goal has been to develop a workflow to i) identify intrusion days throughout the year, ii) classify them into different types, iii) assess their impact *on* and contribution *to* temperature extremes, and iv) evaluate the large-scale conditions in the onset of Saharan intrusions.

https://doi.org/10.5194/egusphere-2024-3331
Preprint. Discussion started: 15 November 2024

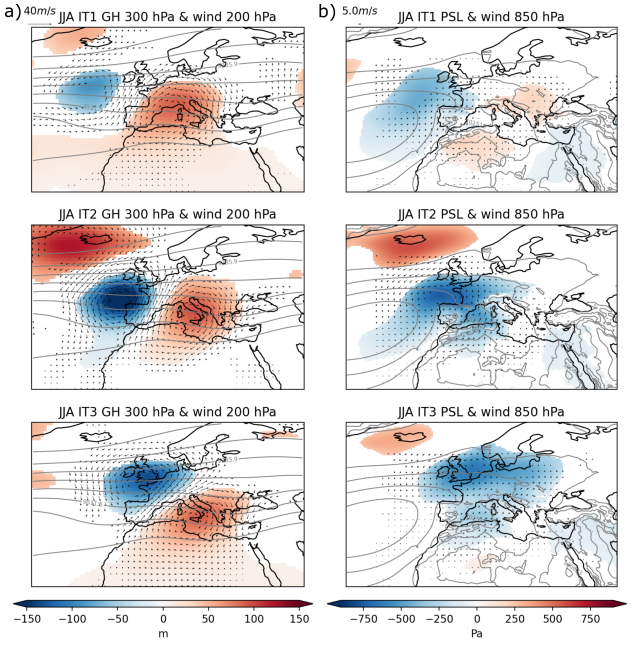

Figure 9. Composites of the first day of the JJA intrusion events for (a) geopotential height (shading) and wind speed (quivers) at 300 hPa and latitudinal wind speed at 850hPa (arrows) and (b) composites of PSL (shading) and wind speed at 850 hPa (quivers) for the three ITs (rows). Anomalies computed with respect to the non-intrusion climatologies of 7-day moving windows centred on each calendar day between 1959-2022. Contours show the climatological 300 hPa geopotential height (a) and PSL (b). No values are shown where the anomaly is not significantly different to 0 with a t-Student test and 95% confidence level.

The method used identifies intrusions of warm air originating in the western Sahara Desert that propagate northward into the WMed. This is achieved through two indicators: the geopotential thickness between 1000 and 500 hPa, and the mean potential temperature between 975 and 750 hPa, following the work by Sousa et al. (2019). These indicators provide insights into the temperature and vertical mixing within the air column—key characteristics of air masses formed in desert regions. The interaction between the land surface and the atmosphere heats the air column, making it highly convective but without cloud formation (Galvin, 2016; Webster, 2020).

During the initial stages of our study, we observed that the tropospheric air properties over the Sahara differ significantly from those of surrounding regions between May and October (warm months). The climatology of the Saharan air masses provides a robust threshold for identifying warm, vertically homogeneous air masses that reach the WMed, as illustrated in Figure 2. Typical Saharan air masses are found to lead to extreme temperatures in the WMed.

A visual inspection of the synoptic situations during all the events revealed that our method successfully captures air masses coming from the Sahara and not with a different origin, increasing our confidence in the method. The atmospheric circulation leading to these intrusions is diverse, often resulting in intrusions confined to spatial scales smaller than the entire WMed. During the cold months, the climatological air masses over the Sahara do not seem exclusive to the Sahara, but rather have

https://doi.org/10.5194/egusphere-2024-3331
Preprint. Discussion started: 15 November 2024

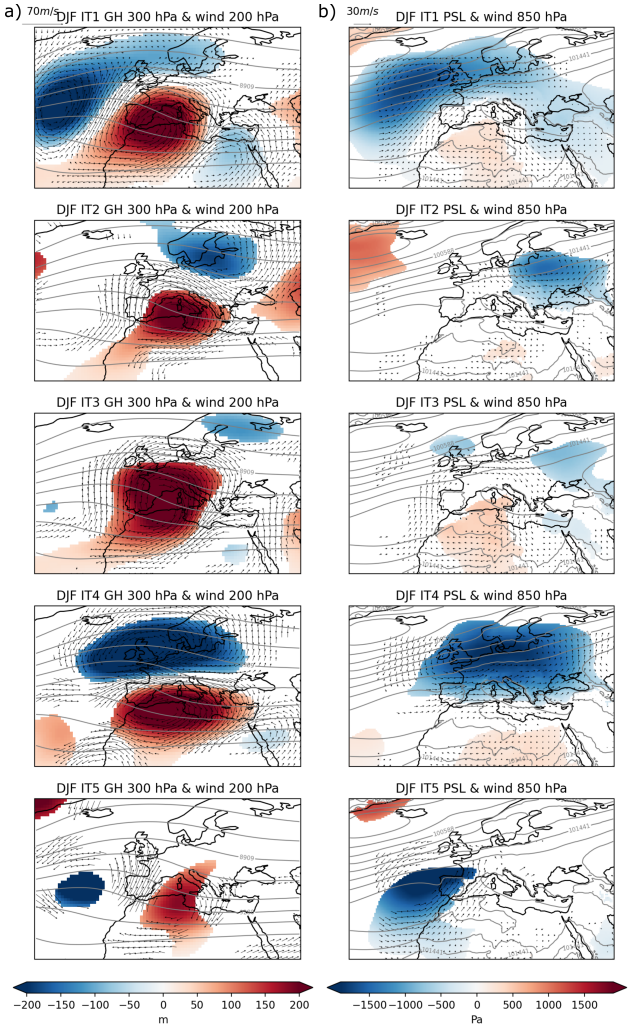

Figure 10. Same as Figure 9 but for the DJF ITs.

similar properties across the latitudinal band. This is due to the reduced influence of the surface radiative balance over desert land that produces the distinctive air mass properties during the warm months. Therefore, we conclude that intrusions during the cold months, though originating from Saharan latitudes, could be similar to subtropical intrusions (Sousa et al., 2021).

This study provides, for the first time, a comprehensive catalogue of Saharan warm air intrusions throughout the year, covering the period from 1959 to 2022. Our approach, while simple and based on just two variables, effectively identifies intrusion events in the WMed. Other studies, some not necessarily focused on the Sahara, have used backward trajectories that may offer greater precision in detecting Saharan air intrusions, though at a significantly higher computational and data volume cost (Lemus-Canovas et al., 2021; Fix et al., 2024). We argue that our computationally cheap workflow can easily be ported to analyse climate model output, which is a key step to evaluate their performance in reproducing this mechanism.

https://doi.org/10.5194/egusphere-2024-3331
Preprint. Discussion started: 15 November 2024

Given that the spatial scale of the intrusions is smaller than the WMed and the visual inspection of the events hinted that intrusions have diverse behaviours, we applied a clustering method to identify distinct intrusion types (ITs). This approach yielded five types for DJF, three for JJA and four for both MAM and SON, each representing the area of influence where the intrusions occur, effectively dividing the study region into subregions. This distinction is relevant because different ITs have varying impacts on regional temperatures and are associated with different large-scale circulations, as discussed below.

While ITs can evolve during a single event, the most common behaviour is for an IT to either maintain its type or transition to a relatively eastern IT, consistent with the prevailing westerly circulation in the region (Olmo et al., 2024). We also observed a significant increase in intrusion days over the historical period in JJA, compatible with long-term thermodynamic changes, such as the warming and expansion of the troposphere, which are linked to global warming (Staten et al., 2018; Webster, 2020; Intergovernmental Panel On Climate Change (Ipcc), 2023). This trend is also reflected in regional observations of extreme heat events in Iberia (Del Río et al., 2011; Cardoso et al., 2019; Fonseca et al., 2016; Sandonis et al., 2021), the Italian peninsula and surrounding islands (Scorzini and Leopardi, 2019; Monforte and Ragusa, 2022; Bey et al., 2024; Caloiero and Guagliardi, 2020), and the broader Mediterranean region (Campos et al., 2024; Cos et al., 2022). Of particular relevance is the summer of the year 2021, when the amount of intrusion days reached 30 days (more than five standard deviations higher than the mean in summer). The summer of 2021 has been studied for its extreme temperatures in the Euro-Mediterranean region (Demirtaş, 2023; Founda et al., 2022).

The historical contribution of Saharan warm air intrusions to extreme temperatures in the WMed is important, especially in JJA. We highlight two key metrics of the relationship between extreme temperatures and intrusions: the impact and contribution. The former is the probability of having an extreme temperature day (TX90p) given that the day is also an intrusion day, and the latter is the probability of having an intrusion day within the sample of TX90p days of a season. The results show that intrusions are very impactful in terms of temperature extremes within their specific cluster type's area of influence, and further north into the EM region (with exception of JJA). In terms of contribution, JJA stands out as the only season with a notable contribution, primarily due to the higher frequency of intrusion events during this period, and can account for around 10% of extreme temperature days. These findings confirm that Saharan intrusions have an important impact on extreme temperatures across all seasons. However, because the frequency of intrusions varies seasonally, only those in JJA make a relevant contribution to overall extreme temperatures. This initial study has not considered the radiative impact of Saharan aerosols to extreme temperatures, as in (Sicard et al., 2022; Cuevas-Agulló et al., 2023), and should be explored in future work.

Through an analysis of anomaly composites for each intrusion type, we identified distinct upper-tropospheric circulation anomalies. The composites of upper tropospheric geopotential show an anomalous high over the area of influence of the ITs, associated with an anomalous circulation around that high that slows down the main flow over Northern Africa. Furthermore, we see that the anomalous high is normally preceded by a westerly shift of positive and/or negative geopotential height centres in the North Atlantic. This pattern holds for all seasons. In some cases, the days leading to the onset of the Saharan intrusion hint at the propagation of an anomaly wavetrain across the North Atlantic. This suggests that there might be an upstream source that forces the anomalous high over the WMed. Some work in this direction but related to other phenomena has been recently conducted by Sandler et al. (2024). They suggest that the connection between upper-level geopotential anomalies and surface

https://doi.org/10.5194/egusphere-2024-3331
Preprint. Discussion started: 15 November 2024

processes in the Mediterranean can originate from Atlantic Ocean sea-surface anomalies. Teng et al. (2022) identify a positive trend in the upper-tropospheric geopotential height in JJA over the EM, associated with an hemispheric wave-like structure forced by the North Atlantic. Therefore, trends in JJA Saharan intrusions could be influenced by the circulation trend described in Teng et al. (2022). This offers an explanation that links the upper troposphere circulation and the Saharan intrusions. Other research has examined the role of the polar jet on extreme temperatures (Rousi et al., 2022; Wang et al., 2013), though the mechanisms behind its fluctuations remain unsolved. Such an analysis of the large-scale dynamics falls beyond the scope of the present work. Further investigation is needed to identify the forcings driving the large-scale circulation anomalies and explore the potential role of teleconnections. Gaining a clearer understanding of these processes could improve the predictability of Saharan warm air intrusions and enhance the evaluation of model simulations, ensuring confidence in their representation of this important phenomenon and its impacts.

Code and data availability. The data used can be accessed through the Climate Data Store maintained by Copernicus at: https://cds.climate.copernicus.eu/datasets.
The code developed to identify the Saharan warm intrusions and to compute all other results of this study can be found at: https://doi.org/10.5281/zenodo.13981589

Author contributions. PC, RM and FD designed the study. PC developed the diagnostics, and wrote the initial manuscript. PC, MO, DC, LP and AM designed the clustering algorithm. All authors contributed to the interpretation and discussion of the results and the improvement of the manuscript.

Competing interests. The contact author has declared that neither they nor their co-authors have any competing interests.

Acknowledgements. We wish to thank all those who have provided the data used for this work and for the data support by M. Samso. The discussions with R. Saurral and J. Mindlin are also gratefully acknowledged. This work was partly supported by the National Research Agency (AEI-Agencia Nacional de Investigación) through the project GLORIA (TED2021-129543B-I00).

https://doi.org/10.5194/egusphere-2024-3331
Preprint. Discussion started: 15 November 2024

References

Alvarez-Castro, M. C., Faranda, D., and Yiou, P.: Atmospheric Dynamics Leading to West European Summer Hot Temperatures Since 1851, Complexity, 2018, 2494 509, https://doi.org/10.1155/2018/2494509, 2018.

Barriopedro, D., García-Herrera, R., Ordóñez, C., Miralles, D. G., and Salcedo-Sanz, S.: Heat Waves: Physical Understanding and Scientific Challenges, Reviews of Geophysics, 61, e2022RG000 780, https://doi.org/10.1029/2022RG000780, 2023.

Bey, E., Türkeş, M., and Hamed, M. M.: Long-term air temperature trends in North Cyprus, Theoretical and Applied Climatology, 155, 1113–1122, https://doi.org/10.1007/s00704-023-04689-6, 2024.

Bladé, I., Liebmann, B., Fortuny, D., and Van Oldenborgh, G. J.: Observed and simulated impacts of the summer NAO in Europe: implications for projected drying in the Mediterranean region, Climate Dynamics, 39, 709–727, https://doi.org/10.1007/s00382-011-1195-x, 2012.

Brogli, R., Kröner, N., Sørland, S. L., Lüthi, D., and Schär, C.: The Role of Hadley Circulation and Lapse-Rate Changes for the Future European Summer Climate, Journal of Climate, 32, 385–404, https://doi.org/10.1175/JCLI-D-18-0431.1, 2019.

Calinski, T. and Harabasz, J.: A dendrite method for cluster analysis, Communications in Statistics - Theory and Methods, 3, 1–27, https://doi.org/10.1080/03610927408827101, 1974.

Caloiero, T. and Guagliardi, I.: Temporal Variability of Temperature Extremes in the Sardinia Region (Italy), Hydrology, 7, 55, https://doi.org/10.3390/hydrology7030055, 2020.

Campos, D. A., Olmo, M. E., Cos, P., Muñoz, A. G., and Doblas-Reyes, F.: Regional aspects of the recent observed trends in the Western Mediterranean: Insights from a Timescale Decomposition Analysis, https://doi.org/10.22541/essoar.172838619.92296453/v1, 2024.

Cardoso, R. M., Soares, P. M. M., Lima, D. C. A., and Miranda, P. M. A.: Mean and extreme temperatures in a warming climate: EURO CORDEX and WRF regional climate high-resolution projections for Portugal, Climate Dynamics, 52, 129–157, https://doi.org/10.1007/s00382-018-4124-4, 2019.

Cherif, S., Doblas-Miranda, E., Lionello, P., Borrego, C., Giorgi, F., Iglesias, A., Jebari, S., Mahmoudi, E., Moriondo, M., Pringault, O., Rilov, G., Somot, S., Tsikliras, A., Vilà, M., and Zittis, G.: First Mediterranean Assessment Report - Chapter 2: Drivers of Change, Tech. rep., MedECC Reports. MedECC Secretariat, Marseille, France., https://doi.org/10.5281/ZENODO.7100601, 2020.

Cos, J., Doblas-Reyes, F., Jury, M., Marcos, R., Bretonnière, P.-A., and Samsó, M.: The Mediterranean climate change hotspot in the CMIP5 and CMIP6 projections, Earth System Dynamics, 13, 321–340, https://doi.org/10.5194/esd-13-321-2022, 2022.

Cramer, W., Guiot, J., Fader, M., Garrabou, J., Gattuso, J.-P., Iglesias, A., Lange, M. A., Lionello, P., Llasat, M. C., Paz, S., Peñuelas, J., Snoussi, M., Toreti, A., Tsimplis, M. N., and Xoplaki, E.: Climate change and interconnected risks to sustainable development in the Mediterranean, Nature Climate Change, 8, 972–980, https://doi.org/10.1038/s41558-018-0299-2, 2018.

Cuevas-Agulló, E., Barriopedro, D., García, R. D., Alonso-Pérez, S., González-Alemán, J. J., Werner, E., Suárez, D., Bustos, J. J., Garcia-Castrillo, G., Garcia, O., Barreto, A., and Basart, S.: Sharp increase of Saharan dust intrusions over the Western Mediterranean and Euro-Atlantic region in winters 2020–2022 and associated atmospheric circulation, https://doi.org/10.5194/egusphere-2023-1749, 2023.

Del Río, S., Herrero, L., Pinto-Gomes, C., and Penas, A.: Spatial analysis of mean temperature trends in Spain over the period 1961–2006, Global and Planetary Change, 78, 65–75, https://doi.org/10.1016/j.gloplacha.2011.05.012, 2011.

Demirtaş, M.: The anomalously hot summer of 2021 over the Euro-Mediterranean region: underlying atmospheric drivers and heatwaves, Theoretical and Applied Climatology, 152, 861–870, https://doi.org/10.1007/s00704-023-04437-w, 2023.

https://doi.org/10.5194/egusphere-2024-3331
Preprint. Discussion started: 15 November 2024

Faranda, D., Messori, G., Jezequel, A., Vrac, M., and Yiou, P.: Atmospheric circulation compounds anthropogenic warming and impacts of climate extremes in Europe, Proceedings of the National Academy of Sciences, 120, e2214525 120, https://doi.org/10.1073/pnas.2214525120, 2023.

Fasullo, J. T. and Trenberth, K. E.: A Less Cloudy Future: The Role of Subtropical Subsidence in Climate Sensitivity, Science, 338, 792–794, https://doi.org/10.1126/science.1227465, 2012.

Fix, F., Mayr, G. J., Zeileis, A., Stucke, I. K., and Stauffer, R.: Atmospheric Deserts: Detection and Consequences, https://doi.org/10.5194/egusphere-2024-2143, 2024.

Fonseca, D., Carvalho, M., Marta-Almeida, M., Melo-Gonçalves, P., and Rocha, A.: Recent trends of extreme temperature indices for the Iberian Peninsula, Physics and Chemistry of the Earth, Parts A/B/C, 94, 66–76, https://doi.org/10.1016/j.pce.2015.12.005, 2016.

Founda, D., Katavoutas, G., Pierros, F., and Mihalopoulos, N.: The Extreme Heat Wave of Summer 2021 in Athens (Greece): Cumulative Heat and Exposure to Heat Stress, Sustainability, 14, 7766, https://doi.org/10.3390/su14137766, 2022.

Galvin, J. F. P.: An introduction to the meteorology and climate of the tropics, MyiLibrary, Wiley Blackwell, Chichester, West Sussex, ISBN 978-1-119-08622-2 978-1-119-08623-9 978-1-119-08624-6, 2016.

Giorgi, F.: Climate change hot-spots, Geophysical Research Letters, 33, 2006GL025 734, https://doi.org/10.1029/2006GL025734, 2006.

Hersbach, H., Bell, B., Berrisford, P., Hirahara, S., Horányi, A., Muñoz-Sabater, J., Nicolas, J., Peubey, C., Radu, R., Schepers, D., Simmons, A., Soci, C., Abdalla, S., Abellan, X., Balsamo, G., Bechtold, P., Biavati, G., Bidlot, J., Bonavita, M., De Chiara, G., Dahlgren, P., Dee, D., Diamantakis, M., Dragani, R., Flemming, J., Forbes, R., Fuentes, M., Geer, A., Haimberger, L., Healy, S., Hogan, R. J., Hólm, E., Janisková, M., Keeley, S., Laloyaux, P., Lopez, P., Lupu, C., Radnoti, G., De Rosnay, P., Rozum, I., Vamborg, F., Villaume, S., and Thépaut, J.: The ERA5 global reanalysis, Quarterly Journal of the Royal Meteorological Society, 146, 1999–2049, https://doi.org/10.1002/qj.3803, 2020.

Horton, D. E., Johnson, N. C., Singh, D., Swain, D. L., Rajaratnam, B., and Diffenbaugh, N. S.: Contribution of changes in atmospheric circulation patterns to extreme temperature trends, Nature, 522, 465–469, https://doi.org/10.1038/nature14550, 2015.

Intergovernmental Panel On Climate Change (Ipcc): Climate Change 2021 – The Physical Science Basis: Working Group I Contribution to the Sixth Assessment Report of the Intergovernmental Panel on Climate Change, Cambridge University Press, 1 edn., ISBN 978-1-00-915789-6, https://doi.org/10.1017/9781009157896, 2023.

Klotzbach, P. J. and Gray, W. M.: Multidecadal Variability in North Atlantic Tropical Cyclone Activity, Journal of Climate, 21, 3929–3935, https://doi.org/10.1175/2008JCLI2162.1, 2008.

Lemus-Canovas, M., Lopez-Bustins, J. A., Martín-Vide, J., Halifa-Marin, A., Insua-Costa, D., Martinez-Artigas, J., Trapero, L., Serrano-Notivoli, R., and Cuadrat, J. M.: Characterisation of Extreme Precipitation Events in the Pyrenees: From the Local to the Synoptic Scale, Atmosphere, 12, 665, https://doi.org/10.3390/atmos12060665, 2021.

Lionello, P. and Scarascia, L.: The relation between climate change in the Mediterranean region and global warming, Regional Environmental Change, 18, 1481–1493, https://doi.org/10.1007/s10113-018-1290-1, 2018.

Martin-Vide, J. and Lopez-Bustins, J.: The Western Mediterranean Oscillation and rainfall in the Iberian Peninsula, International Journal of Climatology, 26, 1455–1475, https://doi.org/10.1002/joc.1388, 2006.

Materia, S., Ardilouze, C., Prodhomme, C., Donat, M. G., Benassi, M., Doblas-Reyes, F. J., Peano, D., Caron, L.-P., Ruggieri, P., and Gualdi, S.: Summer temperature response to extreme soil water conditions in the Mediterranean transitional climate regime, Climate Dynamics, 58, 1943–1963, https://doi.org/10.1007/s00382-021-05815-8, 2022.

https://doi.org/10.5194/egusphere-2024-3331
Preprint. Discussion started: 15 November 2024

Monforte, P. and Ragusa, M. A.: Temperature Trend Analysis and Investigation on a Case of Variability Climate, Mathematics, 10, 2202, https://doi.org/10.3390/math10132202, 2022.

Muñoz, A. G., Goddard, L., Robertson, A. W., Kushnir, Y., and Baethgen, W.: Cross–Time Scale Interactions and Rainfall Extreme Events in Southeastern South America for the Austral Summer. Part I: Potential Predictors, Journal of Climate, 28, 7894–7913, https://doi.org/10.1175/JCLI-D-14-00693.1, 2015.

Muñoz, A. G., Goddard, L., Mason, S. J., and Robertson, A. W.: Cross–Time Scale Interactions and Rainfall Extreme Events in Southeastern South America for the Austral Summer. Part II: Predictive Skill, Journal of Climate, 29, 5915–5934, https://doi.org/10.1175/JCLI-D-15-0699.1, 2016.

Muñoz, A. G., Yang, X., Vecchi, G. A., Robertson, A. W., and Cooke, W. F.: A Weather-Type-Based Cross-Time-Scale Diagnostic Framework for Coupled Circulation Models, Journal of Climate, 30, 8951–8972, https://doi.org/10.1175/JCLI-D-17-0115.1, 2017.

Nabat, P., Somot, S., Mallet, M., Sevault, F., Chiacchio, M., and Wild, M.: Direct and semi-direct aerosol radiative effect on the Mediterranean climate variability using a coupled regional climate system model, Climate Dynamics, 44, 1127–1155, https://doi.org/10.1007/s00382-014-2205-6, 2015.

Olmo, M., Bettolli, M. L., and Rusticucci, M.: Atmospheric circulation influence on temperature and precipitation individual and compound daily extreme events: Spatial variability and trends over southern South America, Weather and Climate Extremes, 29, 100 267, https://doi.org/10.1016/j.wace.2020.100267, 2020.

Olmo, M., Cos, P., Muñoz, A. G., Altava-Ortiz, V., Barrera-Escoda, A., Campos, D., Soret, A., and Doblas-Reyes, F.: Cross-Time-Scale Analysis of Year-Round Atmospheric Circulation Patterns and Their Impacts on Rainfall and Temperatures in the Iberian Peninsula, Journal of Climate, 37, 5525–5541, https://doi.org/10.1175/JCLI-D-23-0735.1, 2024.

Palmer, T. E., McSweeney, C. F., Booth, B. B. B., Priestley, M. D. K., Davini, P., Brunner, L., Borchert, L., and Menary, M. B.: Performance-based sub-selection of CMIP6 models for impact assessments in Europe, Earth System Dynamics, 14, 457–483, https://doi.org/10.5194/esd-14-457-2023, 2023.

Pereira, M. G., Trigo, R. M., Da Camara, C. C., Pereira, J. M., and Leite, S. M.: Synoptic patterns associated with large summer forest fires in Portugal, Agricultural and Forest Meteorology, 129, 11–25, https://doi.org/10.1016/j.agrformet.2004.12.007, 2005.

Regayre, L. A., Deaconu, L., Grosvenor, D. P., Sexton, D. M. H., Symonds, C., Langton, T., Watson-Paris, D., Mulcahy, J. P., Pringle, K. J., Richardson, M., Johnson, J. S., Rostron, J. W., Gordon, H., Lister, G., Stier, P., and Carslaw, K. S.: Identifying climate model structural inconsistencies allows for tight constraint of aerosol radiative forcing, Atmospheric Chemistry and Physics, 23, 8749–8768, https://doi.org/10.5194/acp-23-8749-2023, 2023.

Rousi, E., Kornhuber, K., Beobide-Arsuaga, G., Luo, F., and Coumou, D.: Accelerated western European heatwave trends linked to more-persistent double jets over Eurasia, Nature Communications, 13, 3851, https://doi.org/10.1038/s41467-022-31432-y, 2022.

Rousseeuw, P. J.: Silhouettes: A graphical aid to the interpretation and validation of cluster analysis, Journal of Computational and Applied Mathematics, 20, 53–65, https://doi.org/10.1016/0377-0427(87)90125-7, 1987.

Sandler, D., Saaroni, H., Ziv, B., Tamarin-Brodsky, T., and Harnik, N.: The connection between North Atlantic storm track regimes and eastern Mediterranean cyclonic activity, Weather and Climate Dynamics, 5, 1103–1116, https://doi.org/10.5194/wcd-5-1103-2024, 2024.

Sandonis, L., González-Hidalgo, J., Peña-Angulo, D., and Beguería, S.: Mean temperature evolution on the Spanish mainland 1916-2015, Climate Research, 82, 177–189, https://doi.org/10.3354/cr01627, 2021.

Scorzini, A. R. and Leopardi, M.: Precipitation and temperature trends over central Italy (Abruzzo Region): 1951–2012, Theoretical and Applied Climatology, 135, 959–977, https://doi.org/10.1007/s00704-018-2427-3, 2019.

https://doi.org/10.5194/egusphere-2024-3331
Preprint. Discussion started: 15 November 2024

Seager, R., Osborn, T. J., Kushnir, Y., Simpson, I. R., Nakamura, J., and Liu, H.: Climate Variability and Change of Mediterranean-Type Climates, Journal of Climate, 32, 2887–2915, https://doi.org/10.1175/JCLI-D-18-0472.1, 2019.

Sicard, M., Córdoba-Jabonero, C., Lopez-Cayuela, M.-A., Ansmann, A., Comerón, A., Zorzano, M.-P., Rodríguez-Gómez, A., and Muñoz-Porcar, C.: Aerosol radiative impact during the summer 2019 heatwave produced partly by an inter-continental Saharan dust outbreak – Part 2: Long-wave and net dust direct radiative effect, Atmospheric Chemistry and Physics, 22, 1921–1937, https://doi.org/10.5194/acp-22-1921-2022, 2022.

Sousa, P. M., Barriopedro, D., Ramos, A. M., García-Herrera, R., Espírito-Santo, F., and Trigo, R. M.: Saharan air intrusions as a relevant mechanism for Iberian heatwaves: The record breaking events of August 2018 and June 2019, Weather and Climate Extremes, 26, 100 224, https://doi.org/10.1016/j.wace.2019.100224, 2019.

Sousa, P. M., Barriopedro, D., García-Herrera, R., Woollings, T., and Trigo, R. M.: A new combined detection algorithm for blocking and subtropical ridges, Journal of Climate, pp. 1–64, https://doi.org/10.1175/JCLI-D-20-0658.1, 2021.

Staten, P. W., Lu, J., Grise, K. M., Davis, S. M., and Birner, T.: Re-examining tropical expansion, Nature Climate Change, 8, 768–775, https://doi.org/10.1038/s41558-018-0246-2, 2018.

Tencer, B., Bettolli, M., and Rusticucci, M.: Compound temperature and precipitation extreme events in southern South America: associated atmospheric circulation, and simulations by a multi-RCM ensemble, Climate Research, 68, 183–199, https://doi.org/10.3354/cr01396, 2016.

Teng, H., Leung, R., Branstator, G., Lu, J., and Ding, Q.: Warming Pattern over the Northern Hemisphere Midlatitudes in Boreal Summer 1979–2020, Journal of Climate, 35, 3479–3494, https://doi.org/10.1175/JCLI-D-21-0437.1, 2022.

Thompson, D. W. J. and Wallace, J. M.: The Arctic oscillation signature in the wintertime geopotential height and temperature fields, Geophysical Research Letters, 25, 1297–1300, https://doi.org/10.1029/98GL00950, 1998.

Tuel, A. and Eltahir, E. A. B.: Why Is the Mediterranean a Climate Change Hot Spot?, Journal of Climate, 33, 5829–5843, https://doi.org/10.1175/JCLI-D-19-0910.1, 2020.

Ukkola, A. M., De Kauwe, M. G., Roderick, M. L., Abramowitz, G., and Pitman, A. J.: Robust Future Changes in Meteorological Drought in CMIP6 Projections Despite Uncertainty in Precipitation, Geophysical Research Letters, 47, e2020GL087 820, https://doi.org/10.1029/2020GL087820, 2020.

Urdiales-Flores, D., Zittis, G., Hadjinicolaou, P., Osipov, S., Klingmüller, K., Mihalopoulos, N., Kanakidou, M., Economou, T., and Lelieveld, J.: Drivers of accelerated warming in Mediterranean climate-type regions, npj Climate and Atmospheric Science, 6, 97, https://doi.org/10.1038/s41612-023-00423-1, 2023.

Vogel, M. M., Orth, R., Cheruy, F., Hagemann, S., Lorenz, R., Van Den Hurk, B. J. J. M., and Seneviratne, S. I.: Regional amplification of projected changes in extreme temperatures strongly controlled by soil moisture-temperature feedbacks, Geophysical Research Letters, 44, 1511–1519, https://doi.org/10.1002/2016GL071235, 2017.

Wang, W., Zhou, W., Wang, X., Fong, S. K., and Leong, K. C.: Summer high temperature extremes in Southeast China associated with the East Asian jet stream and circumglobal teleconnection, Journal of Geophysical Research: Atmospheres, 118, 8306–8319, https://doi.org/10.1002/jgrd.50633, 2013.

Webster, P.: Dynamics of The Tropical Atmosphere and Oceans, Wiley, 1 edn., ISBN 978-0-470-66256-4 978-1-118-64846-9, https://doi.org/10.1002/9781118648469, 2020.

Zhang, X., Hegerl, G., Zwiers, F. W., and Kenyon, J.: Avoiding Inhomogeneity in Percentile-Based Indices of Temperature Extremes, Journal of Climate, 18, 1641–1651, https://doi.org/10.1175/JCLI3366.1, 2005.

https://doi.org/10.5194/egusphere-2024-3331
Preprint. Discussion started: 15 November 2024

Zhang, X., Alexander, L., Hegerl, G. C., Jones, P., Tank, A. K., Peterson, T. C., Trewin, B., and Zwiers, F. W.: Indices for monitoring changes in extremes based on daily temperature and precipitation data, WIREs Climate Change, 2, 851–870, https://doi.org/10.1002/wcc.147, 2011.